

# Signaling crosstalk between TGF $\beta$ and Dishevelled/Par1b

A Mamidi<sup>1</sup>, M Inui<sup>1</sup>, A Manfrin<sup>1</sup>, S Soligo<sup>1</sup>, E Enzo<sup>1</sup>, M Aragona<sup>1</sup>, M Cordenonsi<sup>1</sup>, O Wessely<sup>2</sup>, S Dupont<sup>1</sup> and S Piccolo<sup>\*1</sup>

Crosstalk of signaling pathways is critical during metazoan development and adult tissue homeostasis. Even though the transforming growth factor-beta (TGF $\beta$ ) transduction cascade is rather simple, *in vivo* responsiveness to TGF $\beta$  ligands is tightly regulated at several steps. As such, TGF $\beta$  represents a paradigm for how the activity of one signaling system is modulated by others. Here, we report an unsuspected regulatory step involving Dishevelled (Dvl) and Par1b (also known as MARK2). Dvl and Par1b cooperate to enable TGF $\beta$ /bone morphogenetic protein (BMP) signaling in *Xenopus* mesoderm development and TGF $\beta$  responsiveness in mammalian cells. Mechanistically, the assembly of the Par1b/Dvl3/Smad4 complex is fostered by Wnt5a. The association of Smad4 to Dvl/Par1 prevents its inhibitory ubiquitination by ectoderm (also known as transcriptional intermediary factor 1 gamma or tripartite motif protein 33). We propose that this crosstalk is relevant to coordinate TGF $\beta$  responses with Wnt-noncanonical and polarity pathways.

*Cell Death and Differentiation* (2012) 19, 1689–1697; doi:10.1038/cdd.2012.50; published online 11 May 2012

Members of the transforming growth factor-beta (TGF $\beta$ ) growth factors are pleiotropic cytokines that govern multiple cell fate decisions during development, differentiation and tissue homeostasis.<sup>1,2</sup> Defects in TGF $\beta$  responsiveness are common in diseases such as cancer, metastasis and fibrosis.<sup>3,4</sup> The TGF $\beta$  signaling is among the most straightforward signaling cascades: ligand binding to TGF $\beta$  receptors stimulates phosphorylation of receptor-activated Smads (R-Smad), which in complex with Smad4, accumulate in the nucleus and regulate gene expression.<sup>2</sup> This seemingly simple biochemical cascade is the target of intense regulation, mediated, to a large extent, by post-translational modifications and protein–protein interactions that adjust strength and duration of the pathway, or even negate it according to the cellular context.<sup>5</sup> Among these, regulation of Smad4 by a monoubiquitination/deubiquitination cycle recently emerged as a relevant mechanism to set the correct levels of TGF $\beta$  activity *in vivo*.<sup>6,7</sup>

That said, a critical question remains how these layers of regulation are coordinated within other cellular cues. Conceivably, the answer largely relies in how the TGF $\beta$  cascade is modulated by other signaling pathways. A prominent example of this crosstalk is embryonic development, where TGF $\beta$  and Wnt signaling overlap in controlling germ layer patterning, neural induction and morphogenesis.<sup>1,8</sup> Wnt ligands act not only through  $\beta$ -catenin stabilization (i.e., the ‘canonical’ pathway) but also through ‘noncanonical’ pathways; the latter are critical for organization and polarity of epithelia and to orchestrate cell migration, axon growth and gastrulation movements.<sup>9</sup> Integration of Smad activity and canonical Wnt

signaling has received considerable attention.<sup>10–12</sup> Instead, here we explored the crosstalk of TGF $\beta$  with Dishevelled (Dvl) and Par1b, in the context of noncanonical Wnt signaling and and Smad4 regulation.

## Results

**Dvl regulates TGF $\beta$  responses.** We started this investigation by testing if Dvl, shared by canonical and noncanonical Wnt pathways,<sup>9,13</sup> impacts on TGF $\beta$  and bone morphogenetic protein (BMP) signaling. Overexpression of hDishevelled3 (Dvl3) did not activate Smad activity by itself; however, it enhanced the responses to TGF $\beta$  both on the pCAGA12-lux reporter, which is activated by binding of Smad3/Smad4 (Figure 1a) and on pMix2-lux, activated by the Smad2/Smad4 complex (Supplementary Figure S1A). Dvl3 also stimulated the activation of the BMP reporter Id1BRE by BMP-2 (Supplementary Figure S1B). The effect of Dvl3 on pCAGA12-lux and pMix2-lux activation was recapitulated by transfection of rFrizzled2 (Figure 1a and Supplementary Figure S1A), but not by activation of the canonical Wnt/ $\beta$ -catenin pathway, as overexpression of the Wnt-coreceptor LRP6,  $\beta$ -catenin itself, or inhibition of GSK3 did not show enhancement (Supplementary Figure S1C).

Next, we tested whether Dvl is required for Smad activity. Indeed, MDA-MB-231 cells transfected with small interfering RNAs (siRNAs) that deplete all three Dvls (Supplementary Table S1) displayed an attenuated response to TGF $\beta$  or BMP (Figure 1b, compare lanes 2 and 4, and Supplementary Figure S1E). Attesting the specificity of these results,

<sup>1</sup>Department of Biomedical Sciences, University of Padua, Padua, Italy and <sup>2</sup> Cleveland Clinic, Lerner Research Institute, Department of Cell Biology, Cleveland, OH, USA

\*Corresponding author: S Piccolo, Department of Biomedical Sciences, University of Padua, viale Colombo 3, Padua 35100, Italy. Tel: +39 049 8276098; Fax: +39 049 8276079; E-mail: piccolo@civ.bio.unipd.it

**Keywords:** TGF $\beta$ ; Smad activation; Wnt; development

**Abbreviations:** TGF $\beta$ , transforming growth factor-beta; BMP, bone morphogenetic protein; TRIM33, tripartite motif protein 33; Tif1 $\gamma$ , transcriptional intermediary factor 1 gamma; Ecto, ectoderm; GFP, green fluorescent protein; siRNA, small interfering RNA; FCS, fetal calf serum

Received 5.2.12; revised 19.3.12; accepted 20.3.12; Edited by G Melino; published online 11.5.12

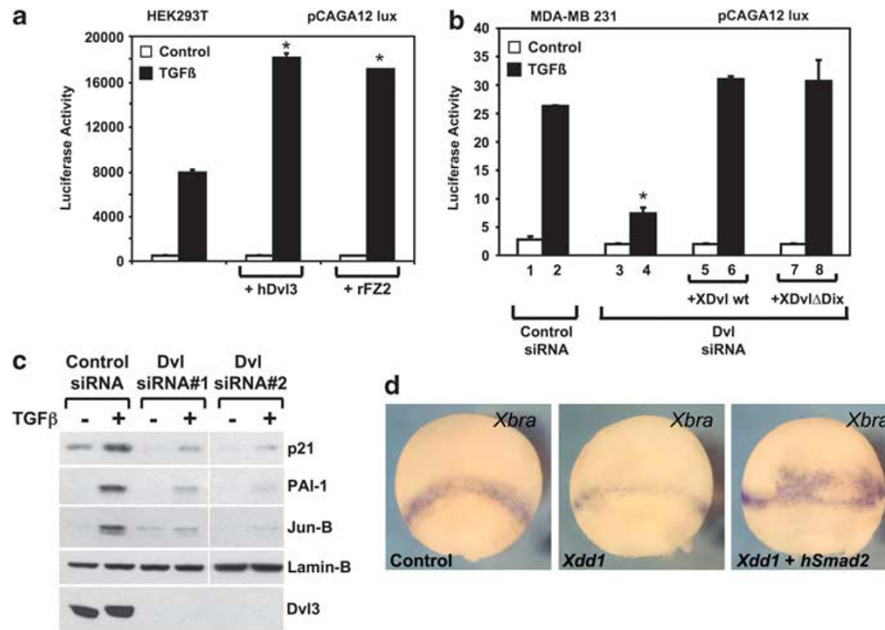


**Figure 1** Dvl is relevant for TGF $\beta$  responses. (a) Graphs show the ligand-mediated inductions of the TGF $\beta$  reporter pCAGA12-lux in HEK293T cells. Raising the levels of Dvl with transfected human Dvl3, or of rFrizzled2 increases TGF $\beta$  transcriptional activity. See Supplementary Figures S1C and D for controls. (b) Treatment with TGF $\beta$  (0.03 ng/ml) of MDA-MB-231 cells transfected with pCAGA12-lux and with control siRNA (lanes 1 and 2) or siRNA-targeting Dvl (lanes 3 and 4, siDvl#1,<sup>36</sup> see Supplementary Table S1). Lanes 5–8 are specificity controls: adding back XDvl or XDvl $\Delta$ Dix rescues TGF $\beta$  transcriptional activity. (c) Immunoblots for p21<sup>Waf1</sup>, JunB and PAI1 whose TGF $\beta$  induction in MDA-MB-231 cells is inhibited by two independent sets of Dvl siRNAs (Supplementary Table S1,<sup>36,37</sup>). LaminB serves as loading controls. Cropped images come from the same exposure of the same blot from which other intervening lanes have been removed. (d) Panels show *in situ* hybridization of *Xenopus* embryos at the gastrula stage stained for the pan-mesodermal marker *Xbra* an *in vivo* read-out of TGF $\beta$ /Nodal signaling. Left panel: uninjected embryo; middle: downregulation of *Xbra* ( $n = 39$ , 64%) in embryos injected at the four-cell stage with 2 ng of *Xdd1* mRNA in the marginal zone. Note that the width of the *Xbra* staining becomes restricted to a narrower band compared to control embryos. Right: rescue by co-injection of *Xdd1* and *Smad2* mRNAs ( $n = 18$ , 67%). See Supplementary Figure S1J for similar requirement of Dvl for BMP responses. Throughout the panel, data are represented as mean and S.D. (\* $P < 0.05$  Student's *t*-test)

the effect of Dvl depletion was rescued by adding back *Xenopus* Dvl (Figure 1b, compare lanes 4 and 6). A rescue was also obtained with a mutant form of Dvl specifically deficient in canonical Wnt/ $\beta$ -catenin signaling, Dvl $\Delta$ Dix<sup>13</sup> (Figure 1b, and Supplementary Figure S1F), suggesting that noncanonical Fz/Dvl signaling is instrumental for TGF $\beta$  and partially for BMP responsiveness (likely acting in concert with the pro-Smad1 effects of Wnt canonical signaling<sup>12</sup>). Importantly, activation of direct endogenous TGF $\beta$  target genes, such as p21<sup>Waf1</sup>, JunB, PAI1 –as well as induction of the BMP-target *ID2* –was attenuated upon Dvl depletion in MDA-MB-231 and Hela cells (Figure 1c and Supplementary Figure S1G and data not shown). These results were confirmed with an independent set of Dvl siRNAs (Figure 1c and data not shown). These data suggest that Dvl is a critical element for TGF $\beta$  responsiveness in diverse cellular contexts.

We next analyzed whether Dvl is also required for TGF $\beta$  responses *in vivo*, by using the *Xenopus* embryo model system. During early development, endogenous TGF $\beta$  and BMP ligands are essential for induction and patterning of the mesodermal germ layer.<sup>1</sup> We inhibited endogenous Dvl function with a Dvl dominant-negative construct, *Xdd1*.<sup>14,15</sup> Embryos were microinjected radially at the four-cell stage with 1 ng of *Xdd1* mRNA and analyzed at the gastrula stage by *in situ* hybridization for the Nodal/Smad-target gene *Xbra*. As shown in Figure 1d, expression of *Xdd1* attenuates *Xbra* activation, and rebalancing TGF $\beta$  signaling by co-injection of *Smad2* mRNA that opposes the effects of *Xdd1* mRNA.

The effect of *Xdd1* is unlikely due to interference with Wnt/ $\beta$ -catenin signaling because depletion of  $\beta$ -catenin with antisense oligonucleotides<sup>16</sup> had no effect on *Xbra* expression (Supplementary Figure S1H) at doses that blocked expression of the Spemann Organizer marker *Chordin*<sup>17</sup> (Supplementary Figure S1I). As for BMP signaling, we monitored expression of the Smad1-target *Sizzled* on the ventral side of the embryo. Dvl knockdown greatly reduced the intensity of the *Sizzled* staining compared with control embryos (Supplementary Figure S1J). Similar results were obtained with *XVent-1*, another direct target of BMP/Smad1 (data not shown). Altogether, these data support the notion that interference with Dvl attenuates TGF $\beta$ /BMP signaling in *Xenopus* embryos, a result in line with data shown above on mammalian cells.

**Par1b regulates TGF $\beta$  responses.** Dvl activity is intimately linked to acquisition of cell polarity, that in turn regulate cell migration and asymmetric organization of the cytoskeleton.<sup>13,18–21</sup> One key element in these events is the interaction between Dvl and Par1b, an evolutionarily conserved kinase of the Par-polarity complex,<sup>22</sup> such that Par1b is essential for noncanonical Wnt/Dvl signaling.<sup>23</sup>

We thus asked if Par1b has a role in the crosstalk between Dvl and TGF $\beta$  signaling in our assays. To assess this, HEK293T and MDA-MB-231 cells were transfected with two independent Par1b siRNAs. We found that endogenous Par1b is relevant for activation of luciferase reporters by TGF $\beta$  and BMP (Figures 2a and b, and data not shown),

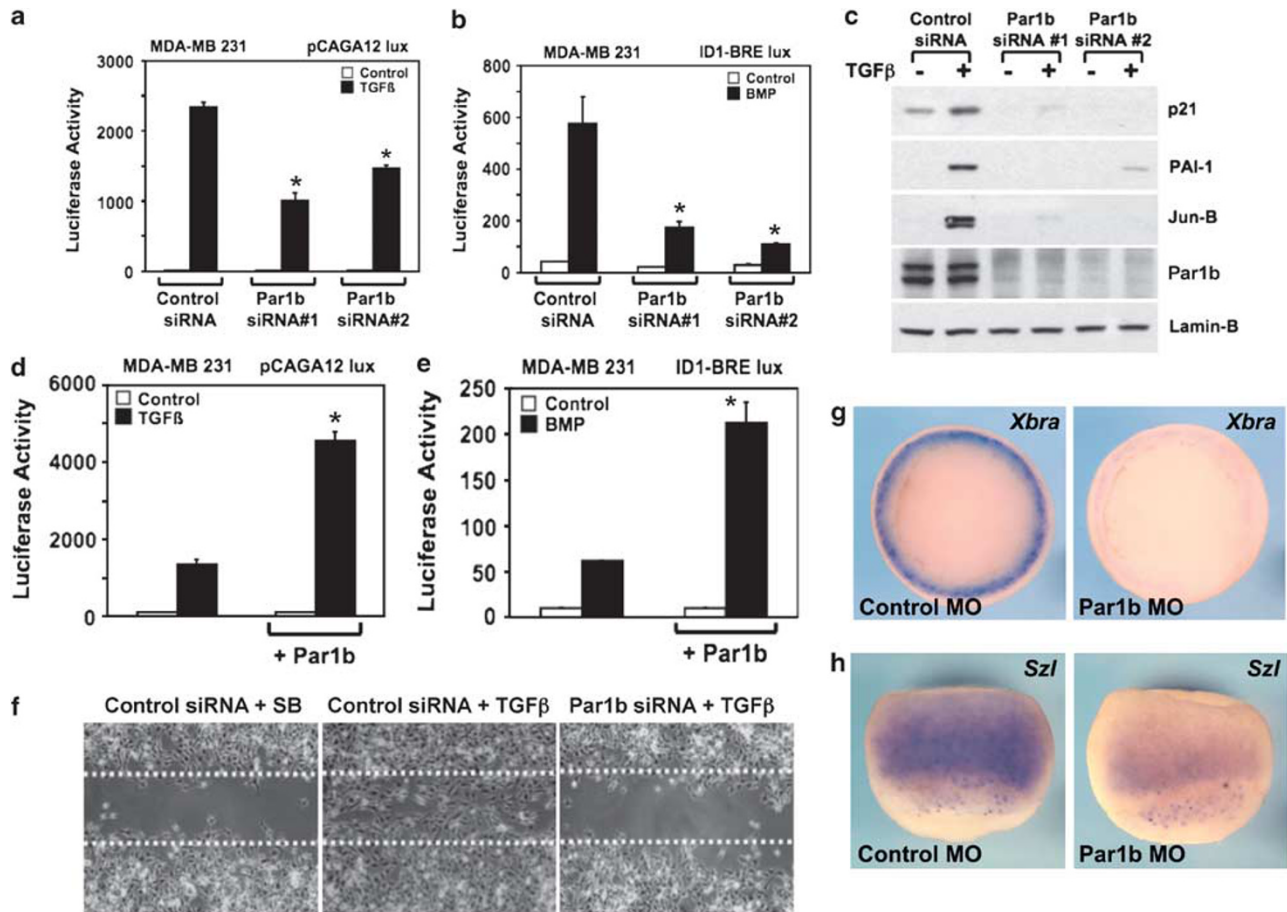


**Figure 2** Par1b is relevant for TGF $\beta$  responses. (a and b) luciferase reporter assays stimulated by TGF $\beta$  (a) or BMP ligands (b) in MDA-MB-231 cells transfected with control or two independent Par1b siRNAs (Supplementary Table S1). Validation of effective knockdown of Par1b was carried prior to luciferase assays (data not shown). (c) Western blot analysis of endogenous TGF $\beta$  targets in control and Par1b-depleted MDA-MB-231 cells. (d and e) luciferase reporter assays stimulated by TGF $\beta$  (d) or BMP (e) ligands and by transfection of Par1b expression vector. (f) Wound-healing migration assay. Panels show representative pictures of MDA-MB-231 cells migrated into a scratch introduced in confluent monolayers. Left: cells transfected with control siRNA and treated with the TGF $\beta$  receptor inhibitor SB431542; middle: migration after 48 h of TGF $\beta$ -treated cells; right: no effect of TGF $\beta$  in Par1b-depleted cells. Dots indicate the edges of the wound at the beginning of the experiment. Quantitations in Supplementary Figure S2C. Similar results were obtained with independent sets of Par1b siRNA. As control, transfection of Par1b siRNAs did not cause any reduction in cell proliferation, as measured by cell counting (data not shown). (g and h) Panels show *in situ* hybridization of *Xenopus* embryos injected with control and anti-Par1b MOs<sup>23</sup> (a mix of 50 ng of Par1 by MO plus 50 ng Par1bx MO) and stained for the TGF $\beta$  target *Xbra* ( $n = 20$ , 100%) (g) and the BMP-target *Sizzled* ( $n = 21$ , 100%) (h), revealing an essential role for Par1b for these inductions. Throughout the panel, data are represented as mean and S.D. (\* $P < 0.05$  Student's *t*-test)

and for induction of endogenous TGF $\beta$  and BMP targets (Figure 2c and Supplementary Figure S2A). This effect was specific for Par1b, as we found no effect upon transfection of the dominant-negative aPKC $\zeta$  isoforms, interfering with the Par6/Par3/aPKC complex (Supplementary Figure S2B). Moreover, overexpression of Par1b in MDA-MB-231 cells synergizes with TGF $\beta$  and BMP ligands in activating their Smad luciferase reporters (Figures 2d and e). In line with these transcriptional effects, Par1b is required for TGF $\beta$ -induced cell migration in wound-healing assays (Figure 2f).

Is Par1b relevant for TGF $\beta$ /BMP responsiveness *in vivo*? Previous studies in *Xenopus* embryos reported a key role for the Dvl/Par1b complex in coordinating gastrulation movements.<sup>23,24</sup> These studies were conducted by microinjecting morpholino (MO) oligonucleotides that individually targeted either XPar1by or XPar1bx, the two *Xenopus* Par1b isoforms. While we reproduced these results (data not shown), we sought to determine the consequences of the combined

depletion of both isoforms. Injection of Par1bx/y MO in cleavage stage *Xenopus* embryos indeed strongly attenuated Nodal-dependent responses, as visualized by *in situ* hybridization for the mesodermal markers *Xbra* and *VegT* (Figure 2g and data not shown). Moreover, Par1b depletion reduced the BMP-dependent inductions of *Sizzled* and *XVent-1* (Figure 2h and Supplementary Figure S2D). We conclude from these experiments that Par1b is required for TGF $\beta$  responses *in vivo*, closely recapitulating the requirements of Dvl in this pathway.

**A Dvl/Par1b/Smad4 complex.** To understand the roles of Dvl and Par1b in TGF $\beta$  responsiveness, we explored the biochemical nature of their requirements. Phospho-Smad3 levels induced by TGF $\beta$  treatment were not quantitatively affected by Dvl or Par1b depletions (Figure 3a, compare lanes 2, 8 and 10). Moreover, TGF $\beta$ -induced degradation of SnoN, a process known to be promoted by receptor

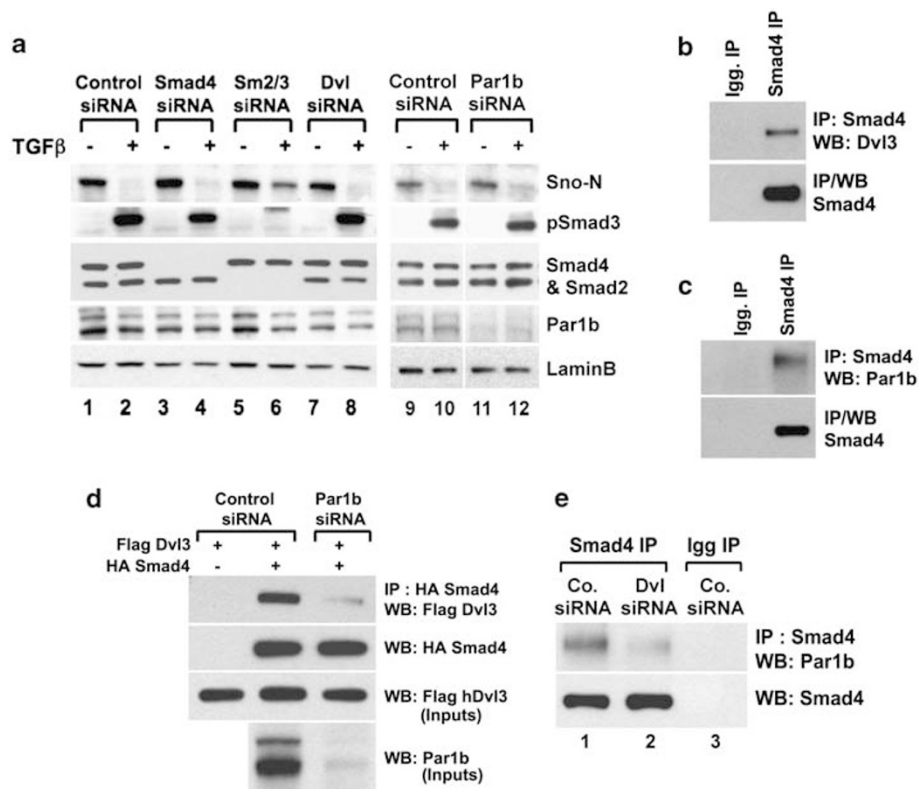


**Figure 3** Dvl and Par1b associate with Smad4 in a mutually dependent manner. (a) Western blot analysis of lysates from cells transfected with the indicated siRNAs, monitoring Smad3 C-terminal phosphorylation downstream of receptor activation and SnoN degradation. The latter is mediated by association between P-Smad2/3 with SnoN in the nucleus, leading to degradation of SnoN independently from Smad4.<sup>6</sup> (b and c) co-IP of Smad4 with Dvl3 (b) or Par1b (c) at endogenous protein levels, from HEK293T cell extracts; control IP was with unrelated IgG. (d) co-IP of Flag-Dvl3 with HA-Smad4 in control or Par1b-depleted HEK293T cells. Hereafter, inputs indicate immunoblots of lysates before co-IP, and serve as control for protein expression or depletion. (e) co-IP of endogenous Par1b and Smad4 proteins from control (lane 1) or Dvl-depleted HEK293T cells (lane 2); lane 3: IP control using an unrelated IgG

phosphorylated Smad2/3 in a Smad4-independent manner,<sup>6</sup> was also not affected by Dvl or Par1b depletion (Figure 3a). These data suggested that TGF $\beta$  receptor activation, R-Smads phosphorylation and their nuclear availability were unlikely primary targets of Dvl/Par1b activity. We thus turned our attention to Smad4. In co-immunoprecipitation (co-IP) experiments from HEK293T cell lysates, Smad4 bound both Par1b and Dvl3 at overexpressed and endogenous protein levels (Figures 3b–d and Supplementary Figure S3A). Dvl and Par1b form a protein complex in multiple cellular contexts, prompting us to investigate the mutual dependency of Par1b and Dvl3 for Smad4 association. Remarkably, depletion of endogenous Par1b impaired Dvl/Smad4 association (Figure 3d) but, at the same time, depletion of endogenous Dvl diminished Par1b/Smad4 complex formation (Figure 3e). To validate such mutual dependency, we assayed the relationships between Par1b and Dvl at the functional level. As shown in Figures 4a and b, overexpression of Dvl3 had no effect on TGF $\beta$ /BMP responsiveness in Par1b-depleted cells; in line, mutation of the Par1b-interaction domain of Dvl3 abolished Dvl3 activity (Supplementary Figure S3B). Interestingly, however, in conditions of protein overexpression, Par1b still displays partial activity in Dvl-depleted cells (Figure 4c). We conclude from these experiments that Par1b and Dvl promote Smad activity by cooperating for Smad4 association, a notion also

supported by co-IP assays where overexpression of Dvl3 enhances Par1b association to Smad4 (Figure 4d).

#### Dvl and Par1b restrain Smad4 monoubiquitination.

Given these biochemical interactions, we initially hypothesized that Par1b might serve as Smad4 kinase. However, in a reconstitution assay of Par1b-depleted cells, a Par1b K49A kinase-dead mutant (Par1b KD) was as efficient as wild-type Par1b in the rescue of TGF $\beta$  responsiveness (Supplementary Figure S3C) indicating a non-enzymatic function of the Dvl/Par1b complex. How then does the binding of Dvl/Par1b to Smad4 regulate Smad activity? Recent loss-of-function studies in mouse and *Xenopus* embryos revealed that a fundamental layer of control for Smad activity centered on Smad4 ubiquitination.<sup>6,7</sup> We hypothesized that Par1b and Dvl may support TGF $\beta$  signaling by preventing Smad4 ubiquitination.<sup>6,7</sup> As shown in Figures 5a and b, Smad4 monoubiquitination was reduced by raising the levels of Dvl3 and Par1b (both wild-type and kinase-dead). This was also observed upon overexpression of Frizzled (Figure 5a), whose effect was further enhanced by co-transfection of noncanonical Wnt ligands, such as Wnt5 and Wnt11 (Supplementary Figure S3D). Conversely, depletion of Par1b from MDA-MB-231 cells (i) increased the levels of Smad4 monoubiquitination (Figure 5c) and (ii) was sufficient to inhibit the effects of Frizzled overexpression (Figure 5d).



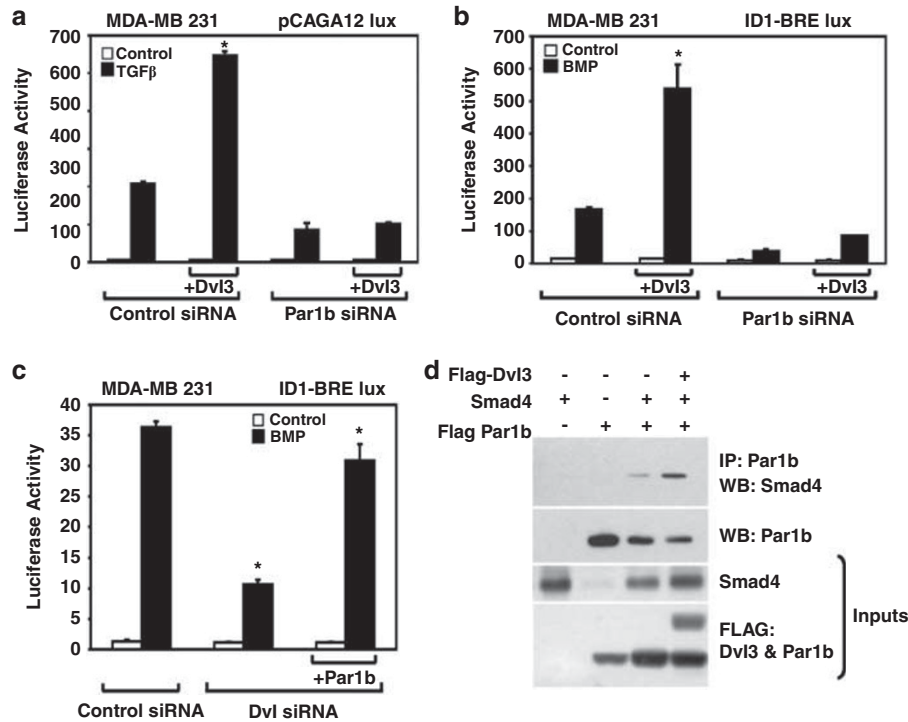


**Figure 4** Dvl works as adaptor of Par1b/Smad4 complex. (a–c) Luciferase assays in MDA-MB-231 cells, showing that overexpression of Dvl3 is unable to stimulate Smad4 activity in cells depleted of Par1b (a and b). However, overexpression of Par1b can foster BMP-activity even in the absence of Dvl (c). Data are represented as mean and SD (\* $P < 0.05$  Student's  $t$ -test). (d) co-IP of overexpressed Par1b and Smad4 (pull down with anti-Par1b antibody) from transfected HEK293T cell lysates with and without co-transfected Dvl3. Co-transfection of Dvl3 enhances Par1b-Smad4 protein interaction

**Par1b/Dvl/Smad4 and Ecto/Smad4 are alternative complexes.** Monoubiquitination of Smad4 is promoted by Ecto/Tif1g/TRIM33 and opposed by the deubiquitinase FAM/USP9x.<sup>6</sup> We first tested if Dvl/Par1b promotes Smad4 deubiquitination through FAM/USP9x, but we found that Par1b or Frizzled were still active in cells depleted of FAM (Supplementary Figure S3E and data not shown); proteasome inhibition was unable to rescue monoubiquitinated Smad4 in Dvl3 or Par1b overexpressing cells (Supplementary Figure S3F and data not shown). We thus tested a different scenario, one whereby Smad4 incorporation in Par1b/Dvl/Smad4 complexes opposes Smad4 interaction with Ecto. This model is supported by the following evidences: (i) endogenous Smad4/Ecto complexes were inhibited upon overexpression of Dvl3 or Par1b (Figure 5e); (ii) *in vitro*, affinity purified Par1b protein antagonizes Smad4/Ecto complexes, and this is enhanced by Dvl3 (Supplementary Figure S3G); (iii) the binding between endogenous Ecto and Smad4 proteins was increased in extracts from Par1b-depleted 293T cells (Figure 5f). These results were validated by using a biochemical read-out of Ecto activity, namely, reduction of the binding between Smad2 and Smad4:<sup>6,25</sup> in agreement with raised levels of Smad4 monoubiquitination, formation of the Smad4/Smad2 complex was decreased in Par1b-depleted cells, and this inhibition could be rescued by the concomitant loss-of-Ecto (Figure 5g). In line with these results, expression of Ecto

inhibits TGF $\beta$  signaling, but this is opposed by co-expression of Dvl3 or Par1b (Figure 5h).

Our observation that Par1b and Dvl foster Smad4 function by opposing Ecto raised an apparent conundrum: to be effective, Par1b and Dvl should act on the same compartment in which Ecto is located, that is, in the nucleus. This is at odd with the general notion that Dvl works in the cytoplasm to regulate Wnt signaling. However, Dvl was also shown to shuttle between the cytoplasm and nucleus<sup>26</sup> such that treatment with the nuclear export (CRM1/exportin) inhibitor leptomycinB causes retention of green fluorescent protein (GFP)-Dvl in the nucleus (see Figure 6b below). Monitoring endogenous Dvl3 localization by nuclear-cytoplasmic fractionation of cell lysates, we detected a nuclear pool of Dvl3 in our cellular systems, which was intriguingly enhanced upon transfection of XWnt5a expression plasmid (Figure 6a, compare lane 1 with lane 3). Similarly, monitoring the localization of Dvl-GFP by immunofluorescence, we also found increased Dvl nuclear residency in Wnt5a-expressing cells (Figures 6b and c). Par1b distribution was even between cytoplasm and nucleus, and not affected by Wnt5a (Figure 6a); however, Wnt5a stimulation increased the formation of the endogenous Par1b/Smad4 complex (Figure 6d) and led to inhibition of Ecto/Smad4 complexes (Figure 6e). Together with data presented in Figure 5, these data suggest that Wnt-noncanonical signaling promotes nuclear Dvl, which, in turn, enhances

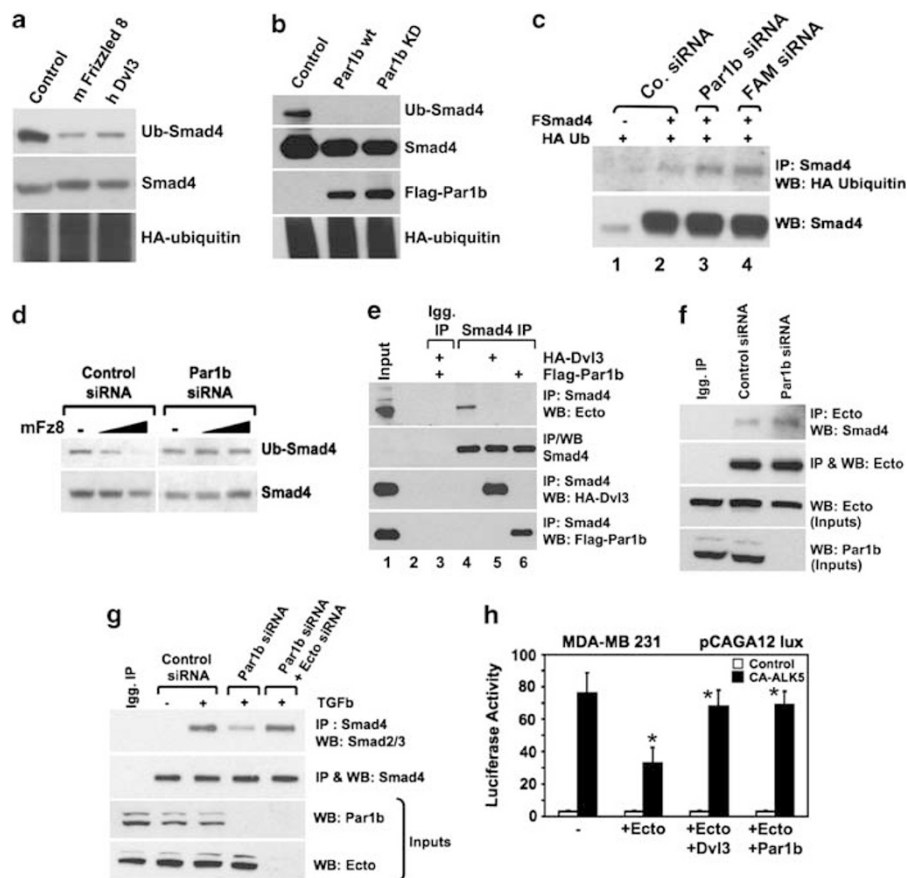


**Figure 5** Dvl and Par1b regulate Smad4 monoubiquitination. (a) Western blot analysis detecting Smad4 monoubiquitination in lysates from HEK293T cells transfected with HA-ubiquitin, Flag-Smad4 and the indicated effectors of the Wnt pathway, that is, mFrizzled8 and hDvl3. Ub-Smad4 is a 75-kDa band reactive to the anti-Smad4 antibody (here shown) and to anti-HA (data not shown; see Dupont *et al.*<sup>6</sup>). (b) Western blot analysis of Smad4 monoubiquitination as in (a) comparing the activity of Par1b wild-type and kinase-dead K49A mutant (40 ng DNA/cm<sup>2</sup>). (c) Anti-Smad4 immunoprecipitation and western blot analysis of lysates of MDA-MB-231 cell transfected with HA-ubiquitin, Flag-Smad4 and the indicated siRNAs. Validation of effective knockdown of Par1b and FAM was carried before ubiquitination assays (data not shown). (d) Smad4 monoubiquitination detected as in (a) in lysates from control and Par1b-depleted cells, transfected with two doses of mFz8 expression vector (5 and 10 ng/cm<sup>2</sup>). (e) co-IPs for Smad4 from HEK293T cells. Endogenous binding of Smad4 to Ecto is inhibited by overexpression of Dvl3 or Par1b. (f) co-IP of endogenous Smad4 and Ecto proteins is enhanced in HEK293T cells depleted of Par1b. (g) co-IP of Smad4 with Smad2/3, monitoring the formation of the active Smad complex, induced by TGF $\beta$  in HEK293T cells transfected with the indicated siRNAs. (h) Dvl and Par1b modulate Ecto activity. Graphs are luciferase reporter assays stimulated by transfection of constitutive-active-TGF $\beta$  receptor (CA-ALK5) in MDA-MB-231 cells in presence of the indicated expression constructs. Data are represented as mean and S.D. (\* $P$  < 0.05 Student's *t*-test)

Par1b/Smad4 complexes at the expenses of the Ecto/Smad4 complexes.

If Par1b works by inhibiting Ecto, then loss-of-Ecto should be epistatic to loss-of-Par1b for TGF $\beta$  responses. We tested this hypothesis in MDA-MB-231 cells with combined siRNA-mediated depletion of Par1b and Ecto. As shown in Figure 7a, loss-of-Ecto readily rescued TGF $\beta$  responsiveness of Par1b-depleted cells. Moreover, also in *Xenopus* embryos, combined depletion of Ecto and Par1b rescued mesoderm deficiency caused by the sole Par1b depletion (Figures 7b and c, compare Par1b MO with Par1b + Ecto MO-injected embryos). Thus, Ecto functions downstream of Par1b.

## Discussion

The data here presented highlight the key role of Ecto/Tif1 $\gamma$ -Smad4 axis as focal point of signaling crosstalk between Dvl/Par1b signaling and TGF $\beta$  ligands. Dvl and Par1b are established regulators of Wnt-noncanonical signaling and cell

polarity.<sup>13,22</sup> Here, we identified a novel function for Dvl and Par1b as positive regulators of the TGF $\beta$ /BMP signaling cascade. We found that formation of a Dvl/Par1b/Smad4 complex protects Smad4 from ubiquitination and inhibition by Ectoderm/Tif1 $\gamma$ . Ecto is an essential negative regulator of TGF $\beta$  gene responses *in vivo*, as validated genetically in Ecto-knockout mice or Ecto-depleted *Xenopus* embryos showing a massive expansion of Nodal/Smad4-induced cell fates.<sup>6,7,27–29</sup> For example, loss of Ecto/TIF1 $\gamma$ /TRIM33 in early mouse embryos leads to aberrant expansion of Nodal targets, such as Lefty or Cerberus, and of Node-associated mesoderm fates in Epiblast-specific Ecto knockouts.<sup>7</sup> Here we propose that by opposing Ecto activity, Dvl/Par1b is required to sustain Smad responsiveness.

An element of novelty in this study is the characterization of a nuclear function for Dvl and Par1b. In canonical and noncanonical Wnt signaling, the function of Dvl takes place either in the cytoplasm or in membrane compartments.<sup>18,19,23</sup> Dvl has also been reported to shuttle through the nucleus,

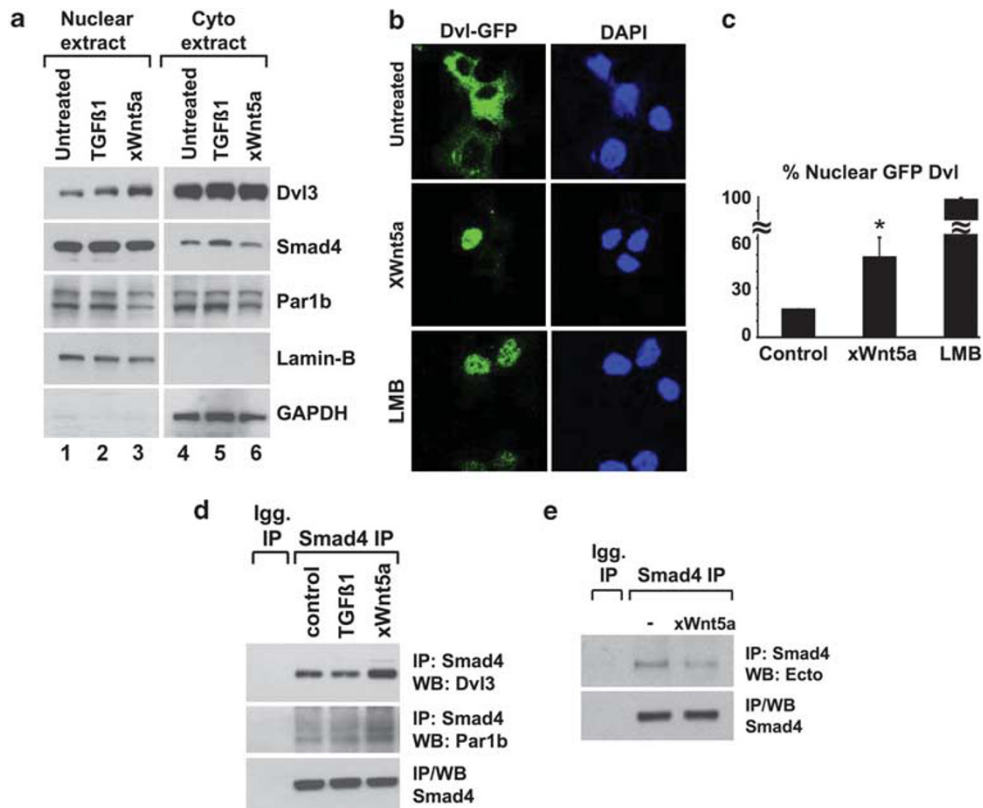


**Figure 6** Wnt5a promotes nuclear Dvl/Par1b/Smad4 complex formation. (a) Monitoring endogenous Dvl3 and Par1b localization by nuclear-cytoplasmic fractionation of HEK293T cell lysates. The nuclear pool of Dvl3 was enhanced upon transfection of XWnt5a (100 ng/cm<sup>2</sup>), whereas Par1b is distributed uniformly between the two compartments. LaminB and GAPDH serve as controls for nuclear and cytoplasmic fractionation. (b) Localization of Dvl-GFP (50 ng/cm<sup>2</sup>) by fluorescence microscopy in HEK293T cells. Note that co-transfection XWnt5a (100 ng/cm<sup>2</sup>) enhances nuclear localization of Dvl-GFP (green channel). Treatment with the nuclear export inhibitor leptomycinB was carried out at 50 ng/ml for 4 h. Hoechst (blue channel) is a nuclear counterstain. (c) Quantification of cells displaying nuclear localization of Dvl-GFP shown in Figure 6b. Transfected cells were fixed and at least seven fields each containing 10–20 GFP-expressing cells were photographed and counted. LMB dramatically shifts Dvl localization into the nucleus (> 95% of cells). Data represent mean and S.D. of two independent experiments. Percentage of nuclear positive Dvl-GFP cells. (d) Endogenous Smad4 interacts with Par1b and Dvl3 from nuclear fractions of HEK293T cells. Wnt5a stimulation increases these nuclear complexes. (e) Endogenous Smad4/Ecto complexes are inhibited in Wnt5a-stimulated HEK293T cells

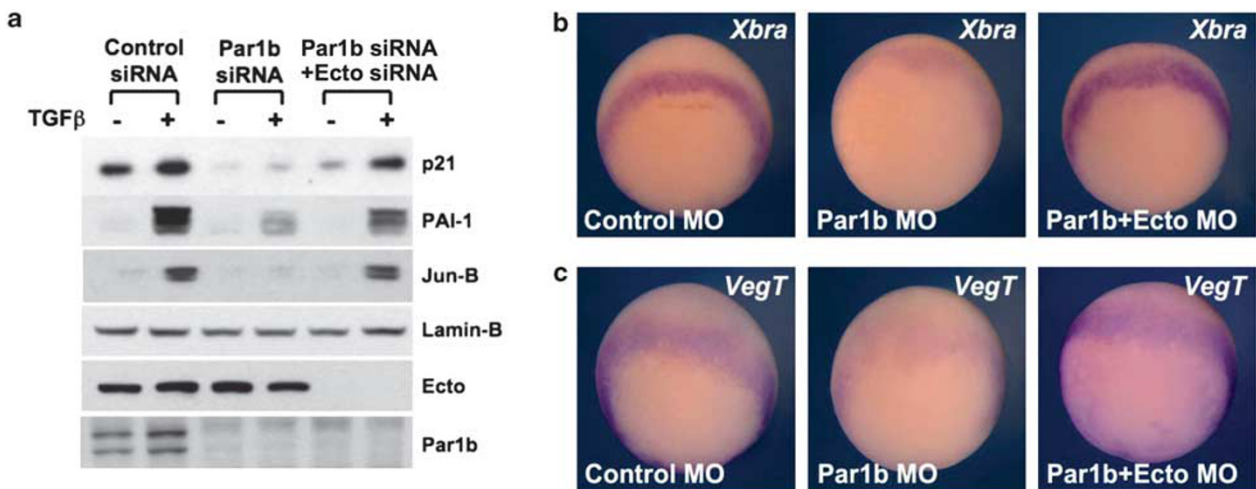


**Figure 7** Ectoderm/Tif1 $\gamma$  is epistatic to Par1b for regulation of TGF $\beta$  signaling. (a) Immunoblots for p21<sup>Waf1</sup>, JunB and PAI1, whose induction by TGF $\beta$  is inhibited by Par1b depletion but rescued by dual depletion of Par1b and Ecto. LaminB serves as loading control. (b and c) Panels show *in situ* hybridization of *Xenopus* embryos injected at the four-cell stage in the marginal zone with control MO (140 ng), Par1b MO (x + y, 80 ng total) alone or in combination with Ecto MO<sup>29</sup> (60 ng). Embryos were stained for *Xbra* and *VegT*. Note that Ecto depletion rescues gene expression in Par1b-depleted embryos ( $n = 22$ , 77% and  $n = 21$ , 67%)

but the biological relevance of this event remained so far poorly understood.<sup>26</sup> Our data suggest that, upon Wnt-noncanonical signaling delivered by Wnt5a, a fraction of Dvl enters (or is stabilized in) the nucleus, where it is engaged in the formation of a complex with nuclear Par1b and Smad4. Indeed, treatment of Wnt5a stabilized the formation of the Dvl/Par1b/Smad4 complex and inhibited Ecto/Smad4 interaction. This parallels with Par1b-dependent inhibition of Smad4 ubiquitination by Frizzled/Wnt5a.

Par1b was originally identified as a Dvl kinase and is also a member of the microtubules-associated regulatory kinases (MARKs).<sup>22,30</sup> Surprisingly, however, our data indicate that the kinase activity of Par1b is actually dispensable for Smad4 activation. This differs from the regulation of TGF $\beta$  signaling by the canonical Wnt pathway, whereby R-Smad-linker phosphorylation is critical for R-Smad ubiquitination and to inhibit TGF $\beta$  responses.<sup>11,12,31</sup>

This work highlights Smad4 as a point for signaling crosstalk in the TGF $\beta$  cascade: it is tempting to speculate that during *Xenopus* mesoderm development, Dvl and Par1b activity may couple and reinforce cell fate specification triggered by TGF $\beta$  ligands with cell polarization and migration. This crosstalk might operate in cellular contexts other than those here investigated. For example, Wnt-noncanonical and TGF $\beta$  pathways have been recently shown to be required and to cooperate in establishing mesenchymal and stem-cell fates in mammary cells, including *de novo* induction of cancer stem cells;<sup>32</sup> this would be consistent with the recently reported requirement of Ecto as endogenous limiting factor for induction of epithelial-to-mesenchymal transition by TGF $\beta$ /Smad4 signaling in immortalized breast cells.<sup>33</sup> Moreover, the activity here described for Dvl and Par1b might also represent either a basal function of these proteins or a function regulated by other signaling cascades, independently of Wnt-noncanonical signals. Dvl and Par1b are indeed key sensors and regulators of cell polarization, adhesion and cytoskeletal dynamics; our findings may represent a mean by which the intensity of TGF $\beta$  responses is harmonized to tissue architecture.

## Materials and Methods

### Biological assays in mammalian cells and *Xenopus* embryos.

**Luciferase assays.** MDA-MB-231 or HEK293T cells were transfected with Transit-LT1 (MirusBio, Madison, WI, USA) and, after 24 h, the medium was changed to 0.2% fetal calf serum overnight. Cells were then either untreated or treated for 8 h with TGF $\beta$ 1 (1 ng/ml, unless indicated otherwise), before harvesting. BMP-2 (Peprotech, Rocky Hills, NJ, USA) was used at 200 ng/ml. Cells were harvested 48 h after transfection. Luciferase reporters CAGA12-luc<sup>34</sup> and ID1-BRE-luc<sup>35</sup> (25 ng/cm<sup>2</sup>) were co-transfected with CMV- $\beta$ -gal (40 ng/cm<sup>2</sup>) to normalize for transfection efficiency with CPRG (Roche, Indianapolis, IN, USA) colorimetric assay. hPar1b/MARK2 and hDvl3 expression plasmids were used at 250 ng/cm<sup>2</sup>. DNA content in all samples was kept uniform by adding pBluescript plasmid. For luciferase assays in siRNA-depleted cells, the indicated siRNAs were transfected first; after 24 h, cells were washed from transfection media, and transfected with plasmid DNA. Unless otherwise indicated, siDvl#1 and siPar1b#1 (see Supplementary Table S1) were used throughout this study. Each sample was transfected in duplicate. Each experiment was repeated three times.

***Xenopus* assays.** *Xenopus* embryo manipulations, capped mRNAs and MO injection and *in situ* hybridization were as previously described.<sup>7</sup> Control MO was 5'-CCTCTTACCTCAGTTACAATTATA-3'; MOs targeting Par1b were as in Ossipova et al.<sup>23</sup> that is, Par1b: 5'-CCAAAAGCAGGTCCTCTCATGTA-3'; Par1 by: 5'-TCGGCAGCGGTGCTCGGTGGTCAT-3'.

All MOs were purchased from Gene Tools (Philomath, OR, USA). MOs were resuspended in HEPES 0.5 mM, pH 7.6 (25  $\mu$ g/ $\mu$ l stock). MOs were heated to 70 °C

for 5 min before microinjection. Embryos at the four-cell stage were microinjected radially in each blastomere with 4 nl, containing a quarter of the per embryo amount of MOs and/or mRNA, and cultivated at 18 °C until reaching the desired developmental stage.

**co-IP and protein ubiquitination assays.** HEK293T and MDA-MB-231 were transfected with combinations plasmid as indicated in each figure. DNA doses were the following: HA-ubiquitin (8  $\mu$ g/10 cm dish), mFZ8 (500 ng/10 cm dish), Flag-Smad4 (100 ng/10 cm dish), Flag-Par1b/MARK2, xFz7, hDvl3, hLRP-6 and AXIN-2, (all at 5  $\mu$ g/10 cm dish). DNA content in each well was kept uniform by adding pBluescript.

For protein-protein interaction studies, cells were treated as indicated and lysed by sonication in lysis buffer (25 mM HEPES (pH 7.8), 400 mM KCl, 5 mM EDTA, 0.4% NP40, 10% glycerol freshly supplemented with 1 mM DTT, protease inhibitor cocktail (Roche), phosphatase inhibitor cocktail II (Sigma, St. Louis, MO, USA), 250 ng/ml ubiquitin-aldehyde (Sigma). Extracts were diluted fourfold to bring KCl concentration to 100 mM and NP40 to 0.1%, supplemented with 5 mM MgCl<sub>2</sub>, and subjected to protein-A sepharose immunoprecipitation 4 h at 4 °C. For ubiquitination assays, cells were harvested 48 h post-transfection by sonication in Ub-lysis buffer (50 mM HEPES (pH 7.8), 200 mM NaCl, 5 mM EDTA, 1% NP40, 5% glycerol, freshly complemented with 1 mM DTT, protease inhibitor cocktail (Roche), phosphatase inhibitor cocktail II (Sigma), and 250 ng/ml ubiquitin-aldehyde (Sigma)). Cell lysates were immunoprecipitated 4 h at 4 °C with protein-A-antibody sepharose beads in Ub-lysis buffer supplemented with 2 mM MgCl<sub>2</sub>, followed by three washes with Ub-wash buffer (50 mM HEPES (pH 7.8), 500 mM NaCl, 1% NP40, 5% glycerol, 1 mM EDTA, 2.5 mM MgCl<sub>2</sub>) each of 2 min rotating at room temperature.

Nuclear and cytoplasmic fractions of HEK293T cells were prepared as follows: confluent cells were washed with PBS and allowed to swell with ice-cold hypotonic buffer (20 mM HEPES at pH 7.6, 20% glycerol, 10 mM NaCl, 1.5 mM MgCl<sub>2</sub>, 0.2 mM EDTA and 0.1% NP40) for 10 min at 4 °C, gently scraped and collected into Falcon tubes. Cells were spun at 500 r.p.m. for 10 min and supernatant was used as the 'cytoplasmic' fraction. The cell pellet was resuspended with Ub-lysis buffer, sonicated and spun and the supernatant was used as 'nuclear' fraction.

## Conflict of Interest

The authors declare no conflict of interest.

**Acknowledgements.** This work is supported by grants from the following agencies: AIRC (Italian Association for Cancer Research) PI and AIRC Special Program Molecular Clinical Oncology '5 per mille', University of Padua Strategic grant, IIT Excellence-grant, HFSP and Comitato Promotore Teletthon grant to SP, and from AIRC and MIUR grants to SD and MC. MI was initially recipient of a Toyobo and Uehara Foundations grants; MI and AM were Marie Curie fellows.

- Niehrs C. Regionally specific induction by the Spemann-Mangold organizer. *Nat Rev Genet* 2004; **5**: 425–434.
- Moustakas A, Heldin CH. The regulation of TGFbeta signal transduction. *Development* 2009; **136**: 3699–3714.
- Adorno M, Cordenonsi M, Montagner M, Dupont S, Wong C, Hann B et al. Mutant-p53/Smad complex opposes p63 to empower TGFbeta-induced metastasis. *Cell* 2009; **137**: 87–98.
- Meulmeester E, Ten Dijke P. The dynamic roles of TGF-beta in cancer. *J Pathol* 2011; **223**: 205–218.
- Lonn P, Moren A, Raja E, Dahl M, Moustakas A. Regulating the stability of TGFbeta receptors and Smads. *Cell Res* 2009; **19**: 21–35.
- Dupont S, Mamidi A, Cordenonsi M, Montagner M, Zacchigna L, Adorno M et al. FAM/USP9x, a deubiquitinating enzyme essential for TGFbeta signaling, controls Smad4 monoubiquitination. *Cell* 2009; **136**: 123–135.
- Morsut L, Yan KP, Enzo E, Aragona M, Soligo SM, Wendling O et al. Negative control of Smad activity by ectoderm/Tif1gamma patterns the mammalian embryo. *Development* 2010; **137**: 2571–2578.
- De Robertis EM, Larrain J, Oelgeschlager M, Wessely O. The establishment of Spemann's organizer and patterning of the vertebrate embryo. *Nat Rev Genet* 2000; **1**: 171–181.
- Lai SL, Chien AJ, Moon RT. Wnt/Fz signaling and the cytoskeleton: potential roles in tumorigenesis. *Cell Res* 2009; **19**: 532–545.
- Eivers E, Demagny H, De Robertis EM. Integration of BMP and Wnt signaling via vertebrate Smad1/5/8 and Drosophila Mad. *Cytokine Growth Factor Rev* 2009; **20**: 357–365.



11. Sapkota G, Alarcon C, Spagnoli FM, Brivanlou AH, Massague J. Balancing BMP signaling through integrated inputs into the Smad1 linker. *Mol Cell* 2007; **25**: 441–454.
12. Fuentealba LC, Eivers E, Ikeda A, Hurtado C, Kuroda H, Pera EM *et al*. Integrating patterning signals: Wnt/GSK3 regulates the duration of the BMP/Smad1 signal. *Cell* 2007; **131**: 980–993.
13. Wallingford JB, Habas R. The developmental biology of Dishevelled: an enigmatic protein governing cell fate and cell polarity. *Development* 2005; **132**: 4421–4436.
14. Wallingford JB, Rowning BA, Vogeli KM, Rothbacher U, Fraser SE, Harland RM. Dishevelled controls cell polarity during *Xenopus* gastrulation. *Nature* 2000; **405**: 81–85.
15. Sokol SY. Analysis of Dishevelled signalling pathways during *Xenopus* development. *Curr Biol* 1996; **6**: 1456–1467.
16. Heasman J, Kofron M, Wylie C. Beta-catenin signaling activity dissected in the early *Xenopus* embryo: a novel antisense approach. *Dev Biol* 2000; **222**: 124–134.
17. Oelgeschlager M, Kuroda H, Reversade B, De Robertis EM. Chordin is required for the Spemann organizer transplantation phenomenon in *Xenopus* embryos. *Dev Cell* 2003; **4**: 219–230.
18. Park TJ, Gray RS, Sato A, Habas R, Wallingford JB. Subcellular localization and signaling properties of dishevelled in developing vertebrate embryos. *Curr Biol* 2005; **15**: 1039–1044.
19. Axelrod JD, Miller JR, Shulman JM, Moon RT, Perrimon N. Differential recruitment of Dishevelled provides signaling specificity in the planar cell polarity and Wingless signaling pathways. *Genes Dev* 1998; **12**: 2610–2622.
20. Witze ES, Litman ES, Argast GM, Moon RT, Ahn NG. Wnt5a control of cell polarity and directional movement by polarized redistribution of adhesion receptors. *Science* 2008; **320**: 365–369.
21. Carmona-Fontaine C, Matthews HK, Kuriyama S, Moreno M, Dunn GA, Parsons M *et al*. Contact inhibition of locomotion *in vivo* controls neural crest directional migration. *Nature* 2008; **456**: 957–961.
22. Goldstein B, Macara IG. The PAR proteins: fundamental players in animal cell polarization. *Dev Cell* 2007; **13**: 609–622.
23. Ossipova O, Dhawan S, Sokol S, Green JB. Distinct PAR-1 proteins function in different branches of Wnt signaling during vertebrate development. *Dev Cell* 2005; **8**: 829–841.
24. Kusakabe M, Nishida E. The polarity-inducing kinase Par-1 controls *Xenopus* gastrulation in cooperation with 14-3-3 and aPKC. *EMBO J* 2004; **23**: 4190–4201.
25. He W, Dorn DC, Erdjument-Bromage H, Tempst P, Moore MA, Massague J. Hematopoiesis controlled by distinct TIF1gamma and Smad4 branches of the TGFbeta pathway. *Cell* 2006; **125**: 929–941.
26. Itoh K, Brott BK, Bae GU, Ratcliffe MJ, Sokol SY. Nuclear localization is required for Dishevelled function in Wnt/beta-catenin signaling. *J Biol* 2005; **4**: 3.
27. Agricola E, Randall RA, Gaarenstroom T, Dupont S, Hill CS. Recruitment of TIF1gamma to chromatin via its PHD finger-bromodomain activates its ubiquitin ligase and transcriptional repressor activities. *Mol Cell* 2011; **43**: 85–96.
28. Levy L, Howell M, Das D, Harkin S, Episkopou V, Hill CS. Arkadia activates Smad3/Smad4-dependent transcription by triggering signal-induced SnoN degradation. *Mol Cell Biol* 2007; **27**: 6068–6083.
29. Dupont S, Zaccagna L, Cordenonsi M, Soligo S, Adorno M, Rugge M *et al*. Germ-layer specification and control of cell growth by Ectoderm, a Smad4 ubiquitin ligase. *Cell* 2005; **121**: 87–99.
30. Sun TQ, Lu B, Feng JJ, Reinhard C, Jan YN, Fantl WJ *et al*. PAR-1 is a Dishevelled-associated kinase and a positive regulator of Wnt signalling. *Nat Cell Biol* 2001; **3**: 628–636.
31. Gao S, Alarcon C, Sapkota G, Rahman S, Chen PY, Goerner N *et al*. Ubiquitin ligase Nedd4L targets activated Smad2/3 to limit TGF-beta signaling. *Mol Cell* 2009; **36**: 457–468.
32. Scheel C, Eaton EN, Li SH, Chaffer CL, Reinhardt F, Kah KJ *et al*. Paracrine and autocrine signals induce and maintain mesenchymal and stem cell states in the breast. *Cell* 2011; **145**: 926–940.
33. Hesling C, Fattet L, Teyre G, Jury D, Gonzalo P, Lopez J *et al*. Antagonistic regulation of EMT by TIF1gamma and Smad4 in mammary epithelial cells. *EMBO Rep* 2011; **12**: 665–672.
34. Dennler S, Itoh S, Vivien D, ten Dijke P, Huet S, Gauthier JM. Direct binding of Smad3 and Smad4 to critical TGF beta-inducible elements in the promoter of human plasminogen activator inhibitor-type 1 gene. *EMBO J* 1998; **17**: 3091–3100.
35. Korchynskyi O, ten Dijke P. Identification and functional characterization of distinct critically important bone morphogenetic protein-specific response elements in the Id1 promoter. *J Biol Chem* 2002; **277**: 4883–4891.
36. Schlange T, Matsuda Y, Lienhard S, Huber A, Hynes NE. Autocrine WNT signaling contributes to breast cancer cell proliferation via the canonical WNT pathway and EGFR transactivation. *Breast Cancer Res* 2007; **9**: R63.
37. Li L, Mao J, Sun L, Liu W, Wu D. Second cysteine-rich domain of Dickkopf-2 activates canonical Wnt signaling pathway via LRP-6 independently of dishevelled. *J Biol Chem* 2002; **277**: 5977–5981.



This work is licensed under the Creative Commons Attribution-NonCommercial-No Derivative Works 3.0 Unported License. To view a copy of this license, visit <http://creativecommons.org/licenses/by-nc-nd/3.0>

Supplementary Information accompanies the paper on Cell Death and Differentiation website (<http://www.nature.com/cdd>)